

TITAN'S UPPER ATMOSPHERE: COMPOSITION AND TEMPERATURE
FROM THE EUV SOLAR OCCULTATION RESULTS

Gerald R. Smith

Earth and Space Sciences Institute, University of Southern California
Tucson Laboratories, Tucson, Arizona 85713

Darrell F. Strobel

Naval Research Laboratory, Washington, D.C., 20375

A. L. Broadfoot, B. R. Sandel, D. E. Shemansky, and J. B. Holberg

Earth and Space Sciences Institute, University of Southern California
Tucson Laboratories, Tucson, Arizona 85713

Abstract. The temperature and composition of the upper atmosphere of Titan have been inferred by observing an occultation of the sun by Titan, using the Voyager 1 ultraviolet spectrometer. The temperature is 176 ± 20 K near the evening terminator and 196 ± 20 K near the morning terminator. The major constituent is N_2 with a density of $2.7 \pm 0.2 \times 10^8$ cm^{-3} at 3840 km. The mixing ratio of CH_4 is $8 \pm 3\%$ at a radial distance of 3700 km near the evening terminator where $[CH_4] \approx 1.2 \times 10^8$ cm^{-3} . On the morning terminator the $[CH_4] \approx 1.2 \times 10^8$ cm^{-3} level is about 20 km lower in the atmosphere. The acetylene mixing ratio above 3400 km is measured at the 1 to 2% level. Below 3300 km it decreases to between 0.1 and 0.3%. A layer of absorbing molecules, possibly polymers, is present at both morning and evening terminators. Near the evening terminator the layer is located between 3350 and 3600 km. Near the morning terminator it is located about 100 km lower in the atmosphere. A simple photochemical model suggests that the homopause is located at 3500 ± 70 km with an eddy diffusion coefficient of 1.2×10^8 cm^2 s^{-1} , which decreases to $\sim 10^8$ cm^2 s^{-1} in the lower stratosphere as $[N_2]^{-2/3}$.

Introduction

Titan has been known to have an atmosphere since the discovery of methane by Kuiper [1944]. The atmosphere was assumed to be tenuous, with a surface pressure of only a few millibars. Later, greenhouse models [Pollack, 1973] along with inversion models [Danielson et al., 1974] were proposed in which methane was the dominant constituent and the surface pressure varied from ten to a few hundred millibars. However, models of the formation of Titan [Lewis, 1971] and a microwave observation of Titan's brightness temperature [Conklin et al., 1977] led Hunten [1977] to argue that Titan may have a thick atmosphere dominated by N_2 with a surface pressure of tens of bars and a surface temperature of 200 K. Except for the presence of CH_4 , little was actually known of the composition and depth of Titan's atmosphere before the Voyager 1 encounter with Saturn.

Results of the Voyager 1 solar occultation by Titan described by Broadfoot et al. [1981] have been analyzed in detail. Previously the data longward of 800 Å were interpreted on the basis of CH_4

absorption alone. We show in the following sections that there is in addition measurable C_2H_2 and probably an absorbing layer very high in the atmosphere. The absorbing layer may be related to the geometric albedo variations described by Caldwell [1974]. The data shortward of 800 Å are consistent with N_2 being the main absorber. The airglow observations confirm that N_2 is the primary constituent [Strobel and Shemansky, this issue].

The Occultation Observation

The Voyager 1 Ultraviolet Spectrometer (UVS) is an objective grating spectrometer covering the wavelength range of 535 to 1700 Å [Broadfoot et al., 1977]. The entire wavelength range is detected simultaneously by a 128-element anode array. The anode array collects the output of a microchannel plate electron multiplier in the image plane of the spectrometer. The capability of changing the electron gain of the microchannel plates allows the detector to operate in a photon-counting mode for dim sources such as airglow or in an analog (current integration) mode for bright sources such as the sun.

For the occultation experiment described here, a small auxiliary entrance aperture offset by 20° from the main aperture was pointed toward the sun while the sun-spacecraft line was well above the atmosphere of Titan, and an unattenuated solar spectrum was recorded. Then as the sun-spacecraft line moved through the atmosphere of Titan at a rate of ≈ 8.9 km/s spectra were recorded every 0.32 s. The transmission of the solar flux through the atmosphere as a function of altitude provided a measure of composition and structure.

The occultation occurred on November 13, 1980, between 0540 and 0600 U.T.. The entrance occultation was at a spacecraft-planet range between 6500 km and 8325 km, and the spacecraft sun line crossed the limb at 2.74° north latitude. The diameter of the sun projected into the atmosphere during entrance was about 8 km and was imaged on about 2 anodes. For the exit occultation the range was greater than 17340 km, at 17.5° south latitude, and the diameter of the sun in the atmosphere was about 17 km. The geometry of the entrance occultation was therefore much more favorable, although both observations were successful. In this paper we rely mainly on data from the entrance occultation; all data shown are from the entrance unless noted otherwise. All al-

Copyright 1982 by the American Geophysical Union.

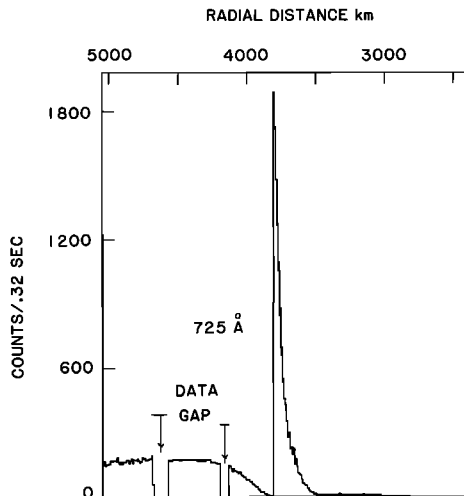


Fig. 1. Signal rate in the 725 Å channel versus radial distance from Titan's center. Absorption of sunlight by Titan's atmosphere causes the decrease in signal that begins at about 4300 km. An automatic gain change increased the signal rate from near zero to over 1800 counts/spectrum at 3810 km. The marked data gaps were caused by a change in spacecraft data rate.

titudes and ranges quoted are referenced to Titan's center.

The occultation measurements were made with a preprogrammed instrument gain change based on signal rate in order to extend the altitude range over which useful measurements could be made. The strategy involved using a lower gain state (HV2) to observe the unattenuated solar flux in the wavelength range shortward of Ly α . When the atmosphere had absorbed most of this flux, a higher gain state (HV3) was used to continue the short wavelength measurements, and to make measurements at wavelengths longward of Ly α , where the sensitivity of the instrument is lower. Figure 1 shows

a plot of signal rate versus altitude that is typical of the short wavelength region. The gain change appears in Figure 1 as a sharp step in signal rate from ≈ 10 to ≈ 2000 . The pre- and post-gain change data were related by using data from a solar calibration sequence in which the instrument scanned across the sun once in the low electron gain state (HV2) and once in the higher electron gain state (HV3). It was then possible to calibrate signal saturation and threshold effects and relate HV2 signal rates to HV3 signal rates over most of the wavelength range shortward of 1200 Å. We assumed that there was no variation in solar output over the time of the solar calibration, ≈ 10 -20 min. The two scans were positioned in wavelength [see Broadfoot et al., 1977] by aligning the solar Ly α line so that individual channels could be related directly. The results of the gain change calibration are shown in Figure 2 for the 725 and 1151 Å channels. Comparison of Figure 1 and Figure 2 shows a satisfactory calibration was obtained. However, in some locations the time period just before the gain change (HV2 \rightarrow HV3) has a very low count rate and no correction can be made. This accounts for the scatter in the scaled data just prior to the gain change.

In the HV3 gain state some wavelengths in the unattenuated solar spectrum are at or near signal saturation. Those areas in saturation must be modeled in order to retrieve the information since the instrument has not measured the actual flux. The conversion from signal rates to photon rates at the instrument requires a nonlinear correction caused by saturation effects in HV3 and threshold effects at the low HV2 gain setting.

The primary uncertainties in the data are due to three factors: (1) The uncertainty in the unattenuated solar flux (I_0) level, (2) the relationship between the signal rates in the HV2 and HV3 data and the relationship of the photo-event rates to the signal rate, and (3) the scattering of the Ly α line within the instrument [see Shemansky et al., 1979]. The greatest uncertainty is probably

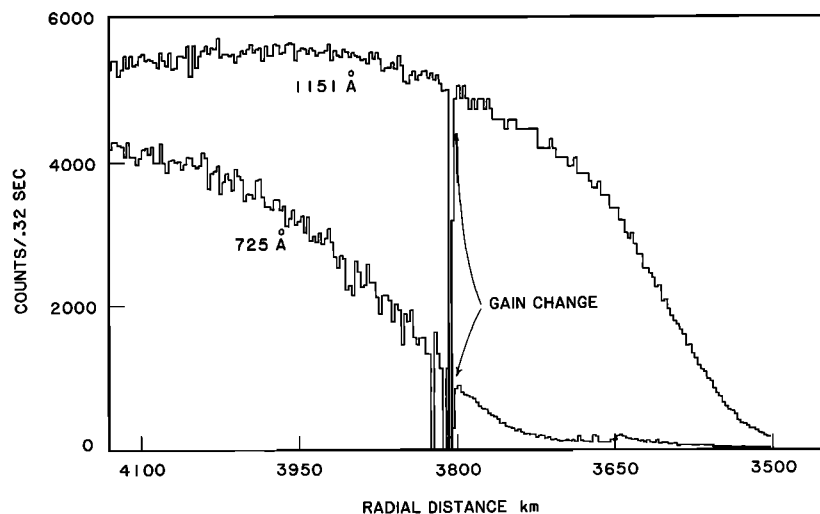


Fig. 2. Absorption curves for the 725 and 1151-Å channels are shown where we have scaled the HV2 gain state data. The gain change location is marked. Above this altitude the HV2 data has been modified so that a continuous absorption curve results. The data below the gain change are unmodified.

due to (3), especially in wavelengths longer than 1216 Å. This is because the instrument is count limited, or saturated, at Ly α and thus the effects of scattering of Ly α cannot be removed using the usual matrix operators [Shemansky et al., 1979].

Short Wavelength Region, λ < 800 Å

The transmitted intensity (I) is given by the equation

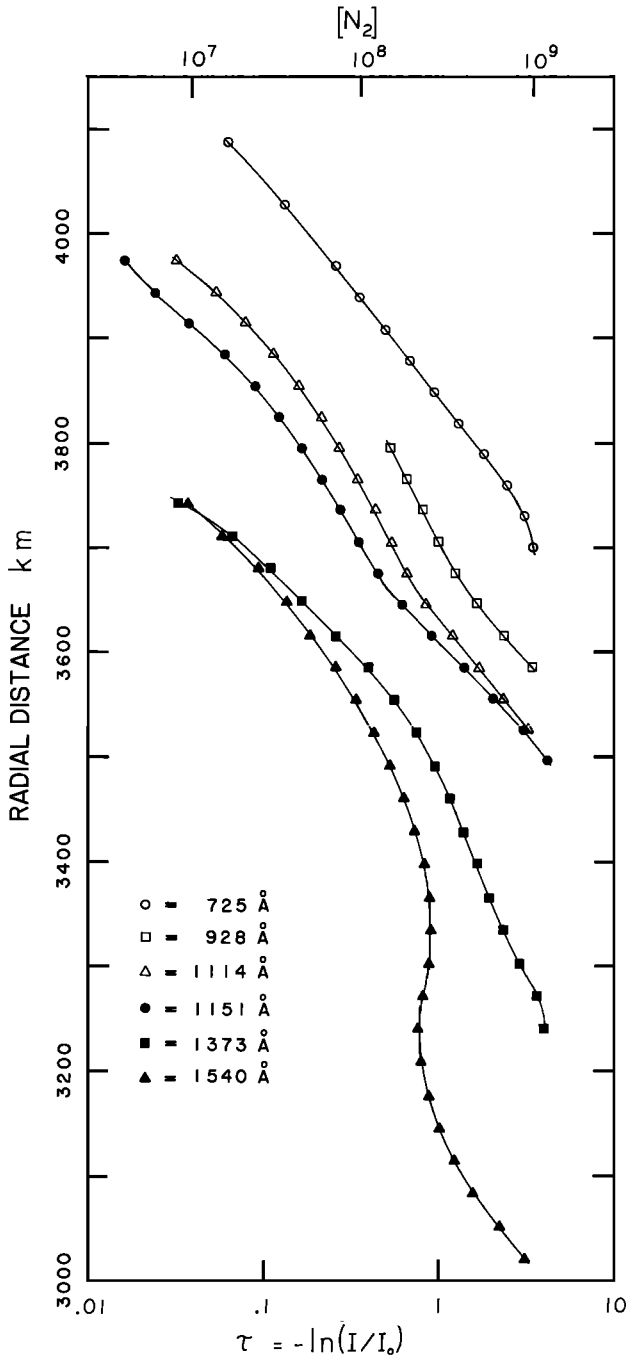


Fig. 3. Optical depth τ at six wavelengths as a function of radial distance from the center of Titan. The lines represent a smooth curve through the data points. The N₂ density scale refers only to the 725 Å curve. The optical depth scale refers to all the curves.

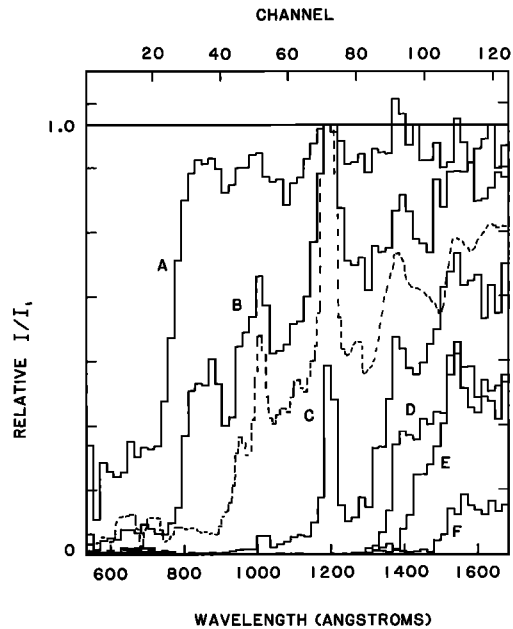


Fig. 4. Relative I/I₁ spectra are shown for various altitudes in the atmosphere, where I₁ is taken from the region (3800 km) just after the gain change from HV2 to HV3. Each spectrum represents a different altitude in the atmosphere as follows: A = 3730 km, B = 3620 km, C = 3500 km, D = 3310 km, E = 3220 km, and F = 3050 km. The dashed curve is taken from model A explained in the text (≈ 1% C₂H₂) and corresponds to an altitude between curves B and C.

$$I = I_0 \exp(-\tau_\lambda) \quad (1)$$

where I₀ is the unattenuated solar intensity and τ_λ is the optical depth of the medium at the wavelength λ. Figure 3 shows -ln(I/I₀) = τ versus altitude for the entrance occultation. We have shown the 725 Å channel as characteristic of this region. The N₂ density scale refers only to this curve. The short wavelength channels indicate τ = 1 at 3840 km ± 10 km, with a scale height of 85 ± 10 km. The corresponding values for the exit occultation are τ = 1 at 3840 ± 10 km and a scale height of 95 ± 10 km. Examination of several areas in the N₂ absorption region showed that the τ = 1 altitude fell well within the 20 km error limit given. A 15% error in I₀ due to internal scattering gives a 20 km error in the determination of the τ = 1 altitude. We feel therefore that the 20 km error given is a reasonable value.

In order to evaluate temperature and density we must decide on what molecular or atomic constituent is doing the absorbing. In Figure 4 we show relative I/I₁ spectrum from the entrance occultation for different levels in the atmosphere. The data are shifted shortward in wavelength about 10 Å due to the displacement of the sun from the center of the slit [see Broadfoot et al., 1977]. The sharp onset of absorption at about 800 Å, could be due to nitrogen or argon [Crudace et al., 1974] but the airglow data show that N₂ is the major constituent [Strobel and Shemansky, this issue]. We therefore interpret the data in this wavelength range in terms of absorption by N₂.

The appropriate equations for the variation of

density with altitude and for the column amount of gas in the line of sight are given by Chamberlain [1963] (appendix). Since the N_2 cross section is not precisely known in the region of 700 Å [see Hudson, 1971; Sullivan and Holland, 1966], we have used a value close to that recommended by Hudson [1971], $2.5 \times 10^{-17} \text{ cm}^2$. For the entrance occultation the temperature at 3840 km is

$$T = 176 \pm 20 \text{ K} \quad (\text{From A2})$$

and the local density of N_2 at this altitude is

$$[N_2] (3840 \text{ km}) = 2.7 \pm 0.2 \times 10^8 \text{ cm}^{-3} \quad (\text{From A1})$$

For the exit the corresponding values are $T = 196 \pm 20 \text{ K}$, $[N_2] (3840 \text{ km}) = 2.6 \pm 0.2 \times 10^8 \text{ cm}^{-3}$. The $\tau = 1$ altitude for N_2 then is at the same altitude on both the entrance and exit. The exit data indicate a slightly higher temperature for the morning terminator. The temperatures given here agree quite well with the values measured at 2760 km by the IRIS experiment [Hanel et al., 1981].

The Region $1200 \text{ Å} > \lambda > 800 \text{ Å}$

In Figure 3 we show $-\ln(I/I_0)$ versus altitude at 1151 and 1114 Å and a portion of the 928 Å channel from the entrance occultation. One characteristic feature of this region is the sharp change in slope, or scale height, at 3660 km. This feature appears in all of the data in this region of the spectrum. The variation occurs within a small fraction of the scale height of the background N_2 . The sharp variation suggests that it is not due to diffusive separation of two constituents, but to the edge of an absorbing layer. The exit data for this region also show a variation in slope but at the slightly lower level of $\approx 3600 \text{ km}$. In the exit data, however, it is not as sharply defined as in the entrance data.

Just above the 3660 km level the change in slope seems to be consistent with CH_4 in diffusive separation at this altitude assuming the temperature is unchanged from the 3840 km level. Therefore the data are interpreted at 3700 km on the entrance occultation as primarily due to CH_4 absorption. Using the absorption at the three wavelengths given above and the absorption cross section of CH_4 ($1.65 \times 10^{-17} \text{ cm}^2$ at 1151 Å, $1.94 \times 10^{-17} \text{ cm}^2$ at 1114 Å, and $5.45 \times 10^{-17} \text{ cm}^2$ at 928 Å) [Hudson, 1971; Mount et al., 1977], we obtain a value of $1.2 \pm 0.4 \times 10^8 \text{ cm}^{-3}$ for the local CH_4 density at 3700 km. The 928 Å data were more heavily weighted since the cross section of CH_4 at 928 Å is nearly three times larger than the values at the other wavelengths. Assuming the atmosphere is isothermal at 176 K in this region gives a value $[N_2] = 1.5 \times 10^8 \text{ cm}^{-3}$ at 3700 km. The mixing ratio is then $[CH_4]/[N_2] = .08 \pm .03$ at 3700 km. The exit data at 3680 km show essentially the same characteristics as the entrance data at 3700 km.

The detection of methane is based primarily on the scale height measured just above 3660 km and the characteristic sharp absorption edge at 1350 Å [Mount et al., 1977]. Ethane also has an edge beginning at about 1350 Å, [Mount and Moos, 1978], but it should have a scale height of about half that of methane.

The Region Longward of 1200 Å

A search for other absorbers was conducted by plotting absorption spectra I/I_1 at several altitudes as shown in Figure 4. The features located at 875, 900, and 1200 Å are due to instrument limiting, or saturation, and are residual solar features, i.e., Ly α at 1216 Å. The absorption features at 1300 Å and at about 1470 Å and the peaks at about 1400 Å and 1550 Å seem to correspond well with the acetylene cross section [Nakayama and Watanabe, 1964]. However, a precise fit is not necessarily expected since the acetylene cross section at 176 K may be quite different from those measured at room temperature, especially in the 1500 Å region where strong bands are located. Acetylene cannot be a dominant minor constituent since the depth of the absorption features below the continuum is small. The dashed curve in Figure 4 is a spectrum calculated from a model having 1% acetylene and corresponding to an altitude between the spectra labeled B and C. The match to the data of the acetylene model is very good, considering the uncertainties in the cross section. Figure 4 also shows that at the 3415 km level the absorption feature at 1430 - 1470 Å disappears, which may indicate a sharp decrease in the acetylene abundance at this altitude. Using the absorption cross section of Lee [1980] for HCN, we have placed an upper limit on the mixing ratio of $[HCN]/[N_2] < 5 \times 10^{-4}$ at an altitude of 3500 km.

In Figure 5 we show a series of absorption curves from 1299 to 1632 Å. We show these data as I/I_1 where I_1 is taken from just after the gain change and is only relative. There is a decrease in absorption with increasing wavelength to 1540 Å, then an increase in absorption at 1623 Å. These data show characteristics of an absorption layer just above 3340 km. The exit occultation data have the same characteristics in this wavelength region. The main difference is that the layer feature occurs at 3200 to 3240 km instead of at 3320 to 3340 km. This feature of the data was originally interpreted by Broadfoot et al. [1981] as an absorption layer. We show in the next section that this interpretation is at least partially correct.

Preliminary Modeling

The data in the region longward of 1200 Å are difficult to analyze directly because of scattering of the Ly α line at 1216 Å within the instrument. The effect of internal scattering can be very large and is difficult to predict without carefully modeling the results since the Ly α line is saturated in the unattenuated solar spectrum. We therefore present simple models based on the above discussion. The instrument response to the solar flux has been modeled by using the known characteristics of the instrument. We have checked this against several Voyager 1 solar calibrations that show an agreement that is quite sufficient for our purposes.

The sun has been modeled by using the Donnelly and Pope [1973] spectrum as a base, updated by fluxes measured in March 1979 by H. E. Hinteregger (personal communication, 1979). The sun was assumed to be a disk of uniform brightness at each wavelength. Since the diameter of the sun

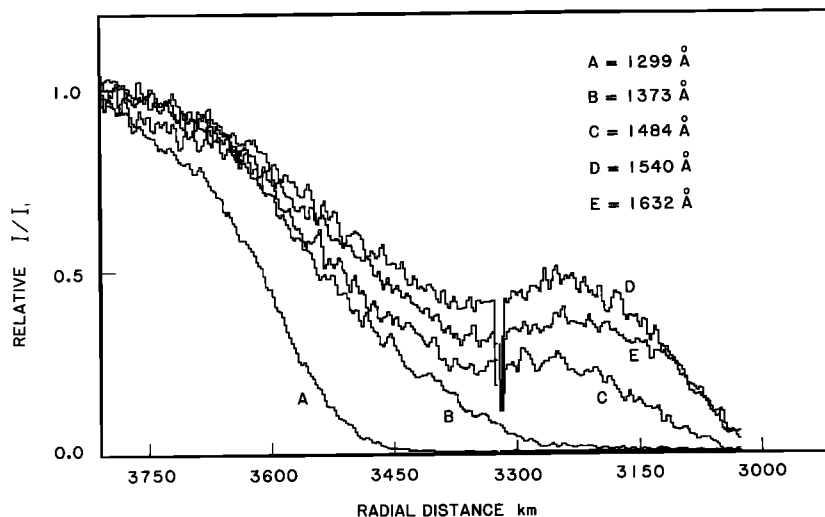


Fig. 5. Relative I/I_1 absorption curves are plotted against radial distance from Titan's center. The data have been smoothed 1-2-1. The feature at 3320 km is a data gap modified by the smoothing process. Each curve represents a different wavelength region where different absorbers dominate. The curve at 1299 Å is where the absorption in methane begins to decrease rapidly with increasing wavelength. Going from 1371 Å to 1540 Å the decrease in attenuation becomes more pronounced.

projected into Titan's atmosphere on entrance is less than 8 km, a departure from uniformity cannot produce a serious error in the analysis.

We present two models differing only in the amount of acetylene present. The models are isothermal at 170 K, with densities at 3840 km of $[N_2] = 3.0 \times 10^8 \text{ cm}^{-3}$, and $[CH_4] = 3.2 \times 10^7 \text{ cm}^{-3}$. The acetylene densities at 3840 km were $[C_2H_2] = 3.6 \times 10^6 \text{ cm}^{-3}$ in model A and $[C_2H_2] = 3.6 \times 10^5 \text{ cm}^{-3}$ in model B. Figure 6 shows the two model results plotted with the data. The model with

$\approx 1\%$ acetylene (model A) fits the 1299 Å absorption curve much better than model B ($0.1\% C_2H_2$). At 1540 Å model A shows an accurate fit down to about 3400 km, whereas model B fits much better below about 3250 km. This seems to indicate that the acetylene content is diminishing rapidly in the lower region as expected from the results of Allen et al. [1980]. The plateau area in the models at 1540 Å is caused primarily by Ly α scattering within the instrument and the absorption of Ly α by CH_4 and C_2H_2 .

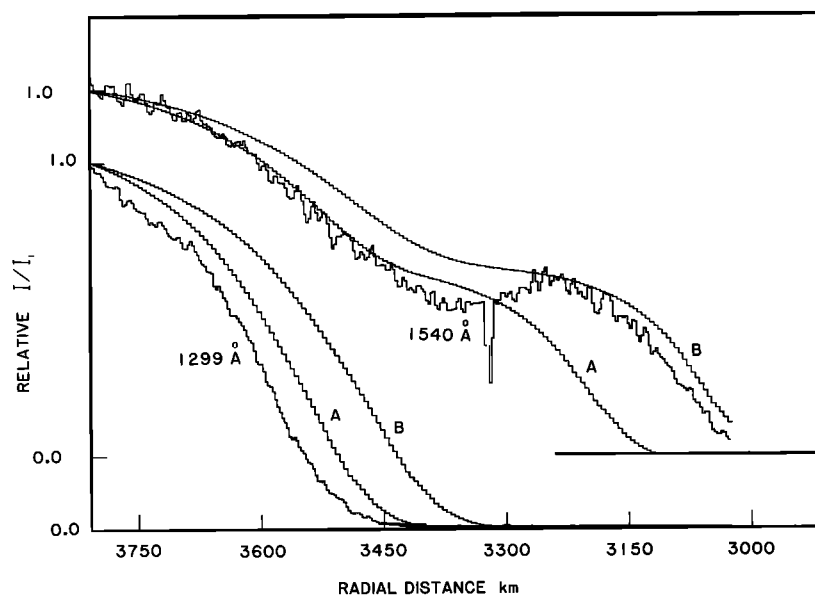


Fig. 6. Relative I/I_1 absorption curves versus radial distance from Titan's center. The data have been smoothed 1-2-1. Both model curves A and B were calculated by assuming an isothermal atmosphere at $T = 170 \text{ K}$, N_2 and CH_4 densities of $3.0 \times 10^8 \text{ cm}^{-3}$, and $3.2 \times 10^7 \text{ cm}^{-3}$ at 3840 km. The two models differ in the C_2H_2 density at that level, having $[C_2H_2] = 3.6 \times 10^6 \text{ cm}^{-3}$ in model A and $[C_2H_2] = 3.6 \times 10^5 \text{ cm}^{-3}$ in model B.

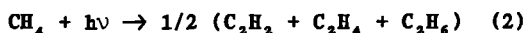
It therefore appears that the layer feature in the data longward of 1400 Å can be explained on the basis of a sharp density decrease of C₂H₂ in the region of 3300–3400 km. We then need about 1 to 2% C₂H₂ above the 3400 km level and 0.1 to 0.3% C₂H₂ below the 3250 km level. This strong variation in C₂H₂ mixing ratio with altitude suggests that polyacetylenes are being produced as discussed by Allen et al. [1980]. The change in slope of the medium wavelength data discussed earlier also suggests that there is a layer of absorbers in the region of 3300 km to 3660 km. Better definition of the parameters will require further detailed model calculations.

Broadfoot et al. [1981] pointed out the existence [see their Figure 6] of a layer located at ≈ 2960 km. This lower layer seems to correspond with the haze layer in the visible images [Smith et al., 1981]. The analysis presented here has not probed that deeply into the atmosphere, and discussion of the lower layer is deferred until further analysis is completed.

Photochemical Interpretation

In order to determine the homopause location and infer the eddy diffusion profile a simple hydrocarbon photochemical model must be constructed. The most recent analysis of Titan's hydrocarbon photochemistry assumed a pure CH₄ atmosphere. Allen et al. [1980] calculated that C₂H₂ was the principal high-altitude product of CH₄ photolysis, whereas at low altitudes C₂H₆ emerged as the predominant hydrocarbon product. Since Titan has an N₂ atmosphere the hydrocarbon chemistry is modified primarily by rapid N₂ quenching of ¹CH₂, produced from CH₄ photolysis, to ³CH₂ with a rate constant of 7.9 × 10⁻¹³ cm³s⁻¹ [Ashford et al., 1980]. At high altitudes, ³CH₂ reacts rapidly with itself to yield C₂H₂; thus the essential features of the Allen et al. [1980] model would not change significantly when applied to an N₂ atmosphere.

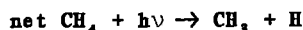
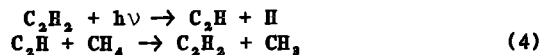
To first order hydrocarbon photochemistry in Titan's N₂ atmosphere can be written as



where the dissociation rate included direct photolysis



and catalytic dissociation of CH₄ [Allen et al., 1980]



For Titan the globally-averaged direct CH₄ photolysis rate is ≈ 1.2 × 10⁹ cm⁻²s⁻¹ at high altitudes, whereas the catalytic dissociation rate is ≈ 6 × 10⁹ cm⁻²s⁻¹ with the assumption of a 0.3 quantum yield for C₂H [Okabe, 1981].

The continuity equations for CH₄ and (C₂H₂ + C₂H₄ + C₂H₆), denoted by subscripts 1 and 2, respectively, are

$$\frac{\partial}{\partial r} (r^2 \phi_1) = -J_1 n_1 r^2 \quad (5)$$

$$\frac{\partial}{\partial r} (r^2 \phi_2) = 1/2 J_1 n_1 r^2 \quad (6)$$

where *n* is number density, *J* is dissociation rate, and ϕ is the vertical flux given by

$$\phi_i = -D_i \left[\frac{\partial n_i}{\partial r} + \frac{n_i}{H_i} \right] - K \left[\frac{\partial n_i}{\partial r} + \frac{n_i}{H_a} \right] \quad (7)$$

Here *K* is the eddy diffusion coefficient, *D_i* is the binary diffusion coefficient in N₂, *H_i* is the scale height of constituent *i*, and *H_a* is the scale height of N₂. The altitude *r₀* is chosen where *D_i* = *K*, the homopause, and

$$D_i = \frac{7.3 \times 10^{16} \text{ T}^{3/4}}{[N_2]} \quad (8)$$

taken from Marrero and Mason [1972] for CH₄ - N₂, and it is assumed to hold for C₂H_x - N₂ also. Titan's upper atmosphere is isothermal and in hydrostatic balance, thus we write

$$[N_2] = [N_2]_0 e^{-(\lambda_a(r_0) - \lambda_a(r))} \quad (9)$$

(see appendix)

From the definition of the homopause $[N_2]_0 = 3.4 \times 10^{18}/K$. From (5) and (6) we note that diffusion is more rapid than dissociation when

$$\frac{H_i^2}{D_i} \ll J_i^{-1} \approx 3 \times 10^7 \text{ s} \quad (10)$$

(cf. Allen et al., [1980] for *J*). Expression (10) holds for N₂ concentrations less than 10¹² cm⁻³ or altitudes greater than 3300 km. Because *J_i* decreases with decreasing altitude as solar photons are absorbed, expression (10) is partially satisfied throughout the atmosphere and to first order (5) and (6) reduce to

$$r^2 \phi_1 = \phi_{10} \quad (11)$$

$$r^2 \phi_2 = \phi_{20} = -1/2 \phi_{10} \quad (12)$$

where ϕ_{10} equals the integrated CH₄ dissociation rate in a radial column.

Integration of (7) and (11) give a general solution for the CH₄ mixing ratio of

$$f_1 = \frac{n_1}{[N_2]} = \frac{n_0}{[N_2]_0} [1 + e^{-(\lambda_a(r) - \lambda_a(r_0))}] (1 - (H_a/H_1)) + \frac{H_{a0} \phi_{10}(r_0)}{[N_2]_0 K (1 - (H_a/H_1))} \quad (13)$$

where $[N_2]_0 K = 3.4 \times 10^{18} \text{ cm}^{-1} \text{ s}^{-1}$, $H/H_1 = 4/7$. For the C_2 hydrocarbons, (7) and (12) are integrated with $H/H_2 = 15/14$ with an average mass of the C_2 hydrocarbons equal to the C_2H_6 mass. While not rigorously correct, the physical representation of the C_2 mixing ratio profile by analytic solutions is more accurate with this assumption. The $T \approx 70$ K cold trap on Titan [Hanel, et al., 1981; Tyler et al., 1981] insures rapid condensation of C_2 hydrocarbons and implies that maximum downward flow is the preferred solution (over the static solution, cf. Strobel [1974]). Hence the C_2H_x mixing ratio is

$$f_2 = \frac{n_2}{[N_2]} = \frac{H_a(r_0) \phi_2(r_0)}{K[N_2]_0 (1-(H_a/H_2))} \quad (14)$$

The appropriate boundary conditions are obtained from the solar occultation data at $r \approx 3700$ km

$$\begin{aligned} f_1 &\approx 0.08 \\ f_2 &\approx 0.016 \end{aligned} \quad (15)$$

and from IRIS results at the base of the thermal inversion layer ($[N_2] \approx 10^{18} \text{ cm}^{-3}$, $r \approx 2650$ km, Hanel et al. [1981], private communication, 1981)

$$\begin{aligned} f_1 &\approx 0.026 \\ f_2 &\approx 5 \times 10^{-5} \end{aligned} \quad (16)$$

Boundary condition (15) implies that C_2H reacts preferentially with C_2H_2 rather than CH_4 , and thus only direct photolysis of CH_4 is important above the homopause. With $\phi_1 = 1.2 \times 10^9 \text{ cm}^{-2} \text{ s}^{-1}$, (13) can be solved with the boundary conditions (15) and (16) and using (12) to yield approximately

$$\begin{aligned} \frac{n_0}{[N_2]_0} &\approx 0.02 \\ r_0 &= 3500 \pm 70 \text{ km} \\ K_0 &= K(r_0) 1.4_{-0.7} \times 10^8 \text{ cm}^2 \text{ s}^{-1} \\ H_a(r_0) &= 67 \pm 3 \text{ km} \end{aligned} \quad (17)$$

The homopause is at ≈ 3500 km with $K_0 \approx 10^8 \text{ cm}^2 \text{ s}^{-1}$. However, the validity of this result depends critically on the boundary conditions, especially when f_1 is almost constant throughout the atmosphere. In order to infer a much lower homopause f_1 at the solar occultation levels would have to be much larger than its value at the base of the thermal inversion layer. The lower boundary condition on f_1 , (16), is also an upper limit because it is based on the cold trap temperature. If f_1 is less than 0.005 (Hunten, 1978), then K_0 would be $< 10^7 \text{ cm}^2 \text{ s}^{-1}$. Substitution of the results (17) and $\phi_2(r_0) = -6 \times 10^8 \text{ cm}^{-2} \text{ s}^{-1}$ into (14) gives $f_2 = 0.016$ in agreement with the solar occultation measurement.

To extend this analysis for $K(r)$ down to the thermal inversion region a $K(r)$ profile shape must be assumed. If, for example,

$$K(r) = K_0 \left(\frac{[N_2]_0}{[N_2]} \right)^\gamma = K_0 e^{-\gamma(\lambda_a(r) - \lambda_a(r_0))} \quad (18)$$

then (6) and (7) can be integrated below the homopause with $D_i = 0$ to yield the maximum downward flow solution

$$f_2 = \frac{H_a(r_0) \phi_2(r_0)}{K_0 [N_2]_0 (\gamma-1)} e^{(\gamma-1)(\lambda_a(r) - \lambda_a(r_0))} \quad (19)$$

where γ is a parameter to be determined. Note that solutions (14) and (19) can be matched at r_0 only with a discontinuity of $(\gamma-1)/(1-(H_a/H_2))$ in either $\phi_2(r_0)$ or f_2 as a consequence of setting $D_i = 0$ to obtain (19). The more plausible case is continuous f_2 , and hence (19) becomes

$$f_2 = \frac{H_a(r_0) \phi_2(r_0)}{K_0 [N_2]_0 (1-(H_a/H_2))} e^{(\gamma-1)(\lambda_a(r) - \lambda_a(r_0))} \quad (20)$$

and reduces to

$$f_2 = \left. \frac{H_a(r_0) \phi_2(r_0)}{K(r_s) [N_2] (1-(H_a/H_2))} \right|_{r_s} \quad (21)$$

at the base of the thermal inversion layer r_s . From the boundary condition (16), (21) can be solved for $K(r_s)$. With $\phi_2(r_0) = -6 \times 10^8 \text{ cm}^{-2} \text{ s}^{-1}$, $H_a(r_0) = 67 \text{ km}$, $[N_2]_{r_s} = 10^{18} \text{ cm}^{-3}$, $K(r_s) \approx 1 \times 10^8 \text{ cm}^2 \text{ s}^{-1}$. The homopause condition, $D_i = K$, is

$$K_0 = K(r_s) \left(\frac{[N_2]_{r_s}}{[N_2]_0} \right)^\gamma \quad (22)$$

and because $K_0 \approx 1 \times 10^8 \text{ cm}^2 \text{ s}^{-1}$, then

$$\gamma \approx 2/3 \quad (23)$$

Thus while the thermal inversion region is as stable and stagnant as the earth's lower stratosphere, Titan's upper atmosphere is vigorously mixed to very high levels. The altitude variation obtained for $K(r)$ is larger than suggested by Lindzen [1971], $\gamma \approx 1/2$, but less than molecular diffusion.

By analogy an HCN mixing ratio of 5×10^{-7} in the thermal inversion layer [Hanel et al., 1981, private communication, 1981] implies a net integrated production rate of $\approx 6 \times 10^6 \text{ cm}^{-2} \text{ s}^{-1}$, approximately a factor of 1000 less than the integrated production rate of N and N^+ . Either conversion of N and N^+ to HCN is inefficient or most HCN produced high in the atmosphere is dissociated before diffusing to the lower atmosphere. Note that the ratio of the HCN mixing ratio to f_2 implies that $f(\text{HCN}) \approx 10^{-4}$ at 3700 km; somewhat below the upper limit determined from the solar occultation data.

Concluding Remarks

The solar occultation data in conjunction with the UVS airglow data conclusively demonstrate that N_2 is the major constituent of Titan's atmosphere.

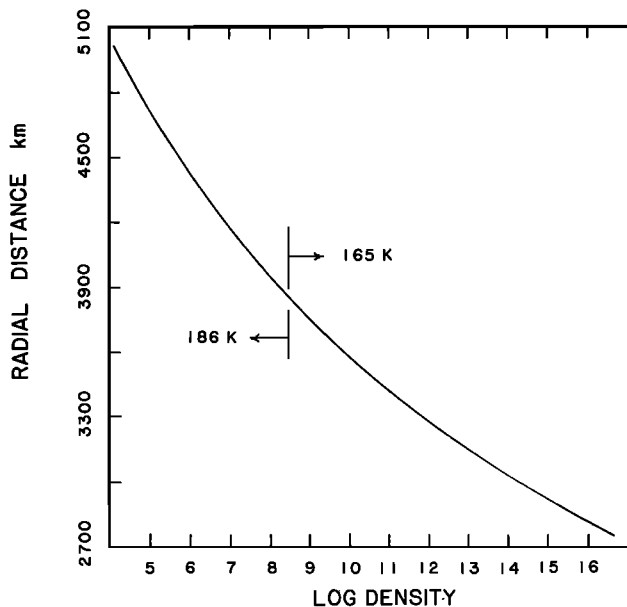


Fig. 7. Model of Titan's N_2 atmosphere as given in the text; log density plotted against radial distance from Titan's center. The areas marked 186 K and 165 K refer to the isothermal temperature used in the model for that altitude region.

From the density variation of N_2 we find that the temperature between 3840 and 4100 km is 186 ± 20 K, approximately 20 K warmer than the thermal inversion region. Although our data suggest that the morning terminator is slightly warmer than the evening terminator, we cannot infer from a direct comparison of the data that this difference is statistically significant.

For engineering purposes an approximate isothermal model atmosphere for Titan can be constructed with expressions (9) and (A2) and the following boundary conditions: $p = 1$ mb, $T = 165$ K, $[N_2]_0 = 4.4 \times 10^{16}$ cm^{-3} at $r_0 = 2750$ km, $H(r_0) = 41.27$ km, and $\lambda(r_0) = 66.63$. This model is valid between 2750 and 3840 km, but the number of significant figures given is not indicative of its accuracy. At 3840 km the boundary conditions change to $[N_2]_0 = 2.7 \times 10^{16}$ cm^{-3} , $T = 186$ K, $H(r_0) = 90.72$ km, and $\lambda(r_0) = 42.33$. Figure 7 shows this model in graphic form. For CH_4 expressions, (13) and (17) should give an adequate altitude profile, although the structure detected at 3660 km is not included.

The relative densities of CH_4 and C_2H_2 above the homopause indicate that C_2H produced from C_2H_2 photolysis will react preferentially with C_2H_2 to form C_4H_2 and initiate the formation of polyacetylenes. This process leads to the destruction of C_2H_2 until a density ratio of C_2H_2/CH_4 is reached where C_2H reacts preferentially with CH_4 to catalytically dissociate CH_4 as illustrated by (4). These essential features of Titan's hydrocarbon density distribution inferred from the solar occultation data were correctly predicted by Allen et al. [1980].

Appendix

The local gravitational acceleration changes rapidly with altitude above Titan. The

appropriate equations used in the text for the column abundance in the line of sight from spacecraft to the sun and for the variation of density with altitude are given below.

$$\eta(r) = n(r) (2\pi r H(r))^{1/2} \left(1 + \frac{9}{8\lambda_i(r)}\right) \quad (\text{A1})$$

$$\text{where } \lambda_i(r) = \frac{GMm_i}{kTr} = \frac{r}{H_i(r)} = \frac{r_0^2}{H_i(r_0)r} \quad (\text{A2})$$

M is the mass of the planet, m_i is the atomic mass of the gas, G is the universal gravitational constant, k is Boltzmann's constant, r is the distance from the planet center, and $H_i(r)$ is the scale height at r . The subscript i refers to the i th constituent, for the background N_2 , $i = a$.

We take $GM = 8.989 \times 10^{28}$ dynes cm^2 gram^{-1} [Anderson et al., 1980]. This gives

$$\lambda_i(r) = 1.087 \cdot 10^{11} \times \left(\frac{A_i}{Tr}\right) \quad (\text{A3})$$

where A_i is the atomic weight of the gas.

At 3800 km, with $T = 170$ K, the values of $\lambda_i(r)$ and the correction term $9/8\lambda_i(r)$ are

	$\lambda_i(r)$	$(9/8 \lambda_i(r))$
N_2	47.12	2.39%
CH_4	26.92	4.18%
C_2H_2	43.75	2.57%

For the vertical distribution of constituent i we used

$$n_i(r) = n_i(r_0) e^{-(\lambda_i(r_0) - \lambda_i(r))} \zeta_i(r) \quad (\text{A4})$$

where we assumed the partition function, $\zeta_i(r)$, was unity.

Acknowledgments. The authors acknowledge the assistance of T. McBreen in processing the Titan occultation data. This work was supported by the Jet Propulsion Laboratory, California Institute of Technology under NASA contract NAS7-100. Additional support was provided by the Planetary Sciences Discipline of NASA's Office of Space Sciences under contract NAGW 161. **NOTE:** The authors point out an error in Figure 6 of Broadfoot et al. [1981]. The altitude scale at the top of the figure has been mislabeled by 100 km; 3000 km should be changed to 3100 km and 4000 km to 4100 km. The values quoted in the text are correct.

The Editor thanks R. E. Hartle and G. H. Mount for their assistance in evaluating this paper.

References

- Anderson, J. D., G. W. Null, E. D. Billerg, S. K. Wong, W. B. Hubbard, and J. J. MacFarlane, Pioneer Saturn celestial mechanics experiment, *Science*, **207**, 449, 1980.
- Allen, M., J. P. Pinto, and Y. L. Yung, Titan: Aerosol photochemistry and variations related to the sunspot cycle, *Astrophys. J. Lett.*, **242**, L125-L128, 1980.

- Ashford, M. N. R., G. Hancock, G. W. Ketly, and J. P. Minshull-Beech, Direct measurements of a ^1A , CH_2 removal rates, J. Photochem., **12**, 75, 1980.
- Broadfoot, A. L., et al., Ultraviolet spectrometer experiment for the Voyager mission, Space Sci. Rev., **21**, 183, 1977.
- Broadfoot, A. L., et al., Extreme ultraviolet observations from Voyager 1 encounter with Saturn, Science, **212**, 206, 1981.
- Caldwell, J. J., Ultraviolet observations of Titan from OAO-2, in The Atmosphere of Titan, NASA SP-340, edited by D. M. Hunten, 1974.
- Chamberlain, J. W., Planetary coronae and atmospheric evaporation, Planet. Space Sci., **11**, 901, 1963.
- Conklin, E. K., B. L. Ulick, J. R. Dickel, 3-mm observations of Titan, Bull. AAS, **9**, 471, 1977.
- Crudace, R., F. Paresce, S. Bowyer, and M. Lampton, On the opacity of the interstellar medium to ultrasoft x-rays and extreme-ultraviolet radiation, Astrophys. J., **187**, 497, 1974.
- Danielson, R. E., J. J. Caldwell, D. R. Larch, An inversion in the atmosphere of Titan, in The Atmosphere of Titan, NASA SP-340, edited by D. M. Hunten, 1974.
- Donnelly, R. F., and J. H. Pope, The 1-3000 Å solar flux for a moderate level of solar activity for use in modeling the ionosphere and upper atmosphere, Tech. Rep. ERL 276-SEL25, NOAA, Boulder, Colo., 1973.
- Hanel, R., et al., Infrared observations of the Saturnian system from Voyager 1, Science, **212**, 192, 1981.
- Hudson, R. D., Critical review of ultraviolet photoabsorption cross sections for molecules of astrophysical and aeronomic interest, Rev. Geophys. Space Phys., **9**, 305, 1971.
- Hunten, D. M., Titan's atmosphere and surface, in Planetary Satellites, edited by J. A. Burns, University of Arizona Press, Tucson, 1977.
- Hunten, D. M., A Titan atmosphere with a surface temperature of 200 K, in The Saturn System, NASA CP-2068, edited by D. M. Hunten and D. Morrison, 1978.
- Kuiper, G. P., Titan: A satellite with an atmosphere, Astrophys. J., **100**, 378, 1944.
- Lee, L. C., $\text{CN}(A^2 \Pi_1 \rightarrow X^2 \Sigma^+)$ and $\text{CN}(B^2 \Sigma^+ \rightarrow X^2 \Sigma^+)$ yields from HCN photodissociation, J. Chem. Phys., **72**, 6414, 1980.
- Lindzen, R. S., Tides and gravity waves in the upper atmosphere, in Mesospheric Models and Related Experiments, edited by G. Fiocco, pp. 122-130, D. Reidel, Hingham, Mass., 1971.
- Lewis, J. S., Satellites of the outer planets: Their physical and chemical nature, Icarus, **15**, 174, 1971.
- Marrero, T. R., and E. A. Mason, Gaseous diffusion coefficients, J. Phys. Chem. Ref. Data, **1**, 3, 1972.
- Mount, G. H., and H. W. Moos, Photoabsorption cross sections of methane and ethane, 1380 - 1600 Å at T=295 K and T=200 K, Astrophys. J. Lett., **224**, L35, 1978.
- Mount, G. H., E. S. Warden, and H. W. Moos, Photoabsorption cross sections of methane from 1400 - 1850 Å, Astrophys. J. Lett., **214**, L24, 1977.
- Nakayama, T., and K. Watanabe, Absorption and photoionization coefficients of acetylene, propyne, and 1-butyne, J. Chem. Phys., **40**, 558, 1964.
- Okabe, H., Photochemistry of acetylene at 1470 Å, J. Chem. Phys., **75**, 2772, 1981.
- Pollack, J. B., Greenhouse models of the atmosphere of Titan, Icarus, **17**, 209, 1973.
- Shemansky, D. E., B. R. Sandel, and A. L. Broadfoot, Voyager observations of the interstellar medium in the 500 to 1700 Å spectral region, J. Geophys. Res., **84**, 139, 1979.
- Smith, B. A., Encounter with Saturn: Voyager 1 imaging science results, Science, **212**, 163, 1981.
- Strobel, D. F., The photochemistry of hydrocarbons in the atmosphere of Titan, Icarus, **21**, 466-470, 1974.
- Strobel, D. F., and D. E. Shemansky, EUV emission from Titan's upper atmosphere: Voyager 1 encounter, J. Geophys. Res., this issue.
- Sullivan, J. O., and A. C. Holland, A congeries of absorption cross sections for wavelengths less than 3000 Å, NASA CR-371, 1966.
- Tyler, G. L., V. R. Eshleman, J. D. Anderson, G. S. Levy, G. F. Lindal, G. E. Wood, and T. A. Croft, Radio science investigations of the Saturn system with Voyager 1: preliminary results, Science, **212**, 202, 1981.

(Received June 8, 1981;

Revised July 27, 1981;

Accepted July 29, 1981.)